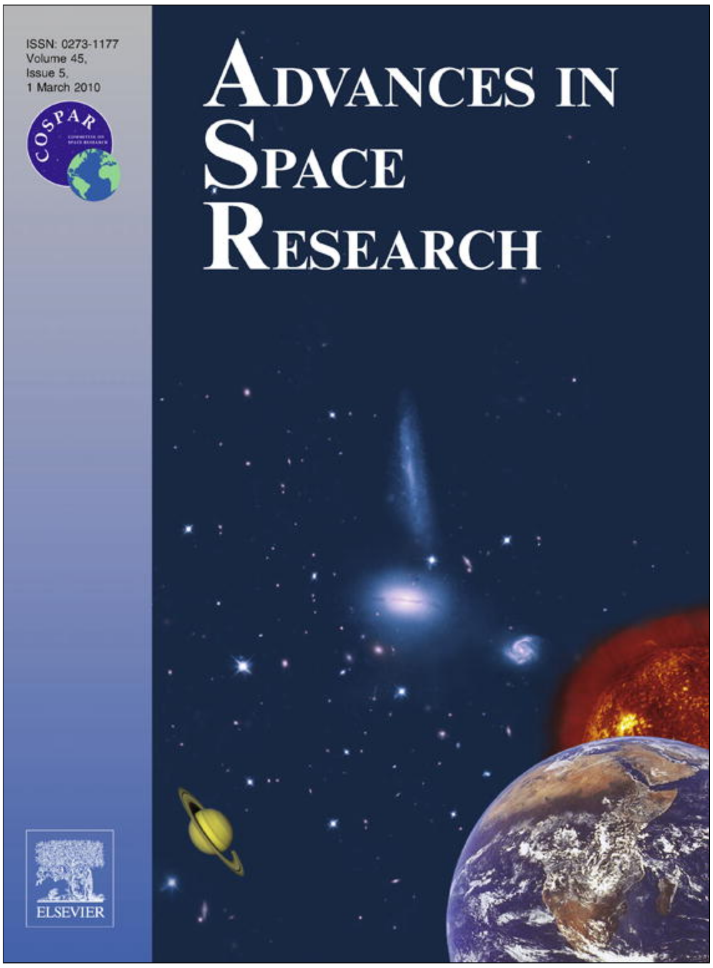
ISSN: 0273-1177
Volume 45,
Issue 5,
1 March 2010
COSPAR
ADVANCES IN
SPACE
RESEARCH
ELSEVIER

Available online at www.sciencedirect.com
ScienceDirect
Advances in Space Research 45 (2010) 614–621
ADVANCES IN SPACE RESEARCH
(a COSPAR publication)
www.elsevier.com/locate/asr

On the relation of the Forbush decreases detected by ASEC monitors during the 23rd solar activity cycle with ICME parameters

A. Chilingarian, N. Bostanjyan *

Cosmic Ray Division, Alikhanyan Physics Institute, Alikhanyan Brothers 2, Yerevan 375036, Armenia

Received 22 April 2009; received in revised form 2 September 2009; accepted 2 September 2009

Abstract

To improve the physical understanding of the Forbush decreases (FD) and to explore the Space Weather drivers, we need to measure as much geospace parameter as possible, including the changing fluxes of secondary cosmic rays. At the Aragats Space Environmental Center (ASEC) are routinely measured the neutral and charged fluxes of secondary cosmic rays. Each of species has different most probable energy of primary "parent" proton/nuclei. Therefore, the energy range of the Galactic Cosmic Rays (GCR) affected by Interplanetary Coronal Mass Ejection (ICME) can be effectively estimated using data of the ASEC monitors. We presented relations of the magnitude of FD observed in different secondary particle fluxes to the most probable energy of the primary protons. We investigate the correlations between the magnitude of FD with the size, speed, density and magnetic field of the ICME. We demonstrate that the attenuation of the GCR flux incident on the Earth's atmosphere due to passing of the ICME is dependent on the speed and size of the ICME and the magnetic field strength.

Keywords: Neutron monitor; Forbush decrease; Interplanetary coronal mass ejection

1. Introduction

The Forbush decreases are the attenuations of the flux of the Galactic Cosmic Rays (GCR) measured by particle detectors on the Earth, on other planets' surfaces and in the interplanetary space before, during and after passage of the Interplanetary Coronal Mass Ejection (ICME). FD takes place in the course of a few hours; over the following several days the GCR intensity returns to pre-FD value.

Using cosmic-ray and magneto-metric measurements Scott Forbush established in 1930s the correlation of worldwide decreases in cosmic-ray intensity with Geomagnetic Storms (GMS, Forbush, 1937). Later he formulated a common geocentric cause for both effects (westward-flowing equatorial ring current as cause of FD (Forbush, 1939)). In 1954 it was recognized that FDs were not produced by the geomagnetic field variations (Simpson, 1954). He claimed on the existence of common mechanism which produces both the accelerating process for cosmic-radiation particles and, indirectly, the geomagnetic disturbances. Examining the relationships among solar activity, GMS, and cosmic-ray intensity, Philip Morrison in 1956 claimed that sporadic emission of clouds of magnetized plasma (now named ICMEs) can modulate the cosmic-ray intensity in interplanetary space and produce terrestrial geomagnetic storms (see Van Allen, 1985 for details).

After establishing that the origin of the non-recurrent FDs are ICMEs and recurrent FDs are caused by the co-rotation of high speed solar wind streams, numerous theoretical and experimental papers were devoted to the possible mechanisms of FD. One of the most intriguing problems was the magnitude of FD. In the paper (Burlaga and Chang, 1988) authors concluded that relatively large decreases in the cosmic-ray intensity are associated with magnetic clouds that are preceded by shocks, whereas only small decreases in CR intensity are associated with magnetic clouds that are not preceded by shocks. Cane

* Corresponding author.
E-mail address: nikolai@yerphi.am (N. Bostanjyan).

0273-1177/$36.00 © 2009 COSPAR. Published by Elsevier Ltd. All rights reserved.
doi:10.1016/j.asr.2009.09.001

(2000) also pointed that 80% of FD with magnitude greater than 4% (in secondary neutron flux) are connected with passage of shock and ejecta. She also claimed that there should be at least two different mechanisms of FD corresponding to the interaction of the GCR with shock and ejecta.

In this paper we made an attempt to research the dependence of the FD magnitude not only on the CME launch helio-coordinates, or existence of the fast shock, but also on the energy of the primary cosmic rays, ICME speed, and ICME density and magnetic field.

In ASEC (Chilingarian et al., 2003, 2005), we measure neutral and charged fluxes by particle detectors located at three different altitudes. Each of the measured secondary fluxes has a different most probable energy of primary "parent" proton/nuclei. As we can see from Fig. 1 (Zazyan and Chilingarian, 2009), these energies range from 7 (mode of distribution of primary protons generated neutrons) to 40 GeV (the same for muons with energies greater than 5 GeV). New particle detectors now starting to operate in ASEC will prolong this maximal energy up to 200 GeV (Chilingarian and Hovsepyan, 2008). Therefore, from the ASEC monitor data we can estimate the GCR energy range affected by ICME and reconstruct actual spectra of the GCRs incident on terrestrial atmosphere, thus revealing the energy-dependant pattern of the ICME modulation effects. Recently analogical techniques were developed for the study of the GCR energy and the FD recovery time (Usoskin et al., 2008), with the difference that data was taken from world-wide networks of Neutron Monitors and three ground level muon telescopes. Measurements of all the secondary fluxes at one and the same location are preferable due to effects of the longitudinal dependence of the FD magnitudes (Haurwitz et al., 1965).

Also we introduce several parameters enumerating the "FD-efficiency" of IMCE, for instance, correlation coefficients between time series of different species of secondary cosmic rays. For small FDs the correlation between changing fluxes of neutrons and 5 GeV muons is small or moderate. We expected that large FDs will influence primary protons of much greater energies comparing with small ones, therefore correlations between fluxes of secondary neutrons and 5 GeV muons will be much greater for large FDs.

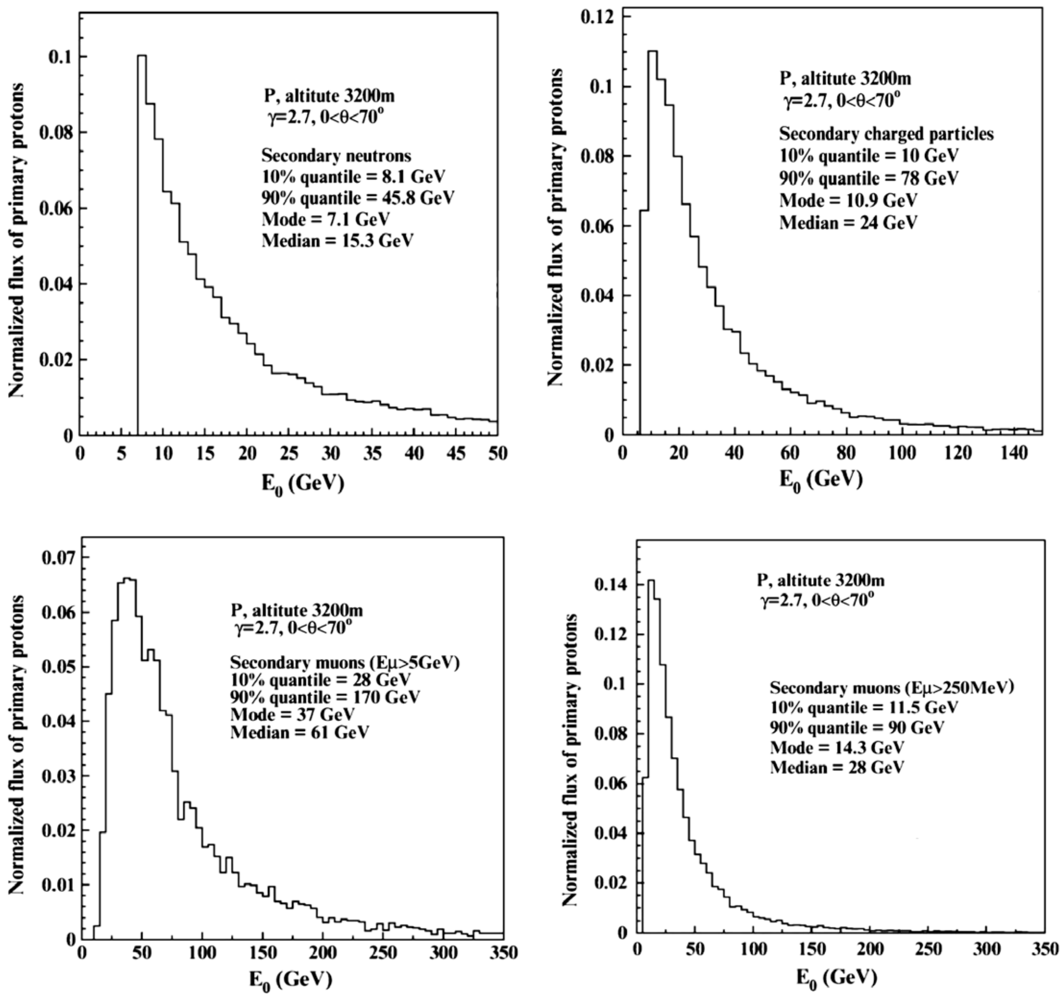

Fig. 1. Energy distribution of the GCR protons initiated various secondary particles at Aragats, 3200 m altitude. The characteristic of the distributions (quintiles, mode, median) helps to estimate most probable energy of each of secondary particle species; the detection efficiency equals to the ratio of primary protons to detected particles.

Another parameter possibly sensitive to ICME modulation strength is the power index of dependence of FD magnitude (percent of flux decrease) on energy of primary protons. Proceeding from a variety of particle detectors at ASEC we can reliably estimate the energy dependence of the attenuation of primary particle flux.

In presented paper we use simple regression model to:

1. Point-up the inter-relations of the FD amplitudes detected in the fluxes of neutrons, low energy charged particles (mostly muons and electrons) and high energy muons. Deduce from it obvious effect that the less is energy of primary particle initiated detected specie of the secondary cosmic ray the greater should be the amplitude of FD.
2. Illustrate the adequateness of the two introduced measures of the FD "strength" based on the detection of FD in different fluxes of secondary particles.
3. Demonstrate the existence or absence of relations between measured FD magnitude and several parameters of the ICME measured by space born facilities.

We still miss the theory and detailed operational models of the propagation of the ICME in the interplanetary space. The interactions of ICME with GCR and magnetosphere can hardly be unfolded in simple models and the observed magnitude of FD is due to complicated interplay of several unknown, or hard to measure parameters, as the ICME size, speed, and magnetic field, as well as conditions of the interplanetary magnetic field and magnetosphere, and other. On present stage of our understanding of these phenomena, simple one-parametric linear models can, at least, outline the relevant characteristics, to be used in future more complicated and more adequate models.

Therefore, the reliability of the obtained relations are done in the terms of values of the determination coefficients R^2, showing how well the regression line represents the data and correlation coefficient R demonstrating the strength of linear connections between two variables. Also the 95% confidence intervals of the correlation coefficients are posted in the figures in the brackets. To prove absence of correlation we post in the figures the, so-called, p-value of the statistical test (particularly Student two-tailed test), which tells us how likely it is that we would get sample correlation coefficient r, just by chance, if there is no correlation at all in the population. If that p-value is very small (usually chosen with a threshold of 0.05), we conclude that the sample correlation is *not* due to chance and the population does have some correlation. If it is not very small (for instance >0.05) we cannot reject hypotheses of "no correlation" and can claim that there is no causal relations between examined variables.

The main disadvantages of linear models is strong sensitivity to the presence of unusual data points in the data used to fit a model. Unfortunately, we are not performing controlled experiments and we are obliged to use the scarce data the nature present us. And, sure, there is some extent of arbitrariness in deciding which correlation is significant and which – not. In the paper the graphicall assess to the data is widely used to demonstrate whether or not linear fits are consistent. In the analysis we accept that a correlation greater than 0.7 is generally described as *strong*, whereas a correlation less than 0.4 is generally described as *weak*. We think that systematically applying the one and the same criteria to rather complicated FD & ICME data we present useful information on the dependences and causal connections of the parameters crucial for the investigated problem.

In the second section we present the selection criteria of the FD events detected by ASEC particle detectors. In the third section the comparison of the ASEC data with muon data from Moscow engineering-physics institute detectors is performed. The forth section is devoted to correlations of FD magnitude with ICME various parameters.

2. Selection of the FD events detected by ASEC

In Table 1 we present selected FD events detected by the ASEC particle detectors during 2002–2006 and introduce indices reflecting the "modulation strength" of the

Table 1
Relative decreases of neutrons, low energy charged particles and high energy muons with energies greater than 5 GeV during FD and the corresponding ICME parameters.

	Relative decrease of neutrons (%)	Relative decrease of charge component (%)	Relative decrease of muons >5 GeV	Correlation coefficient between 1 min time series of neutrons and muons >5 GeV	Power index of the fit of FD magnitude vs primary energy	Maximum speed of solar wind km/s (by ACE, SOHO)
2002.09.07	3.6	2.6	1	0.64	−0.99	570
2003.10.29	20	15	6	0.97	−0.89	>1000
2003.11.20	3.8	2.8	1	–	–	730
2004.01.22	7.5	4	1.3	0.88	−1.26	690
2004.07.27	10	7	3	0.97	−0.88	1000
2004.11.09	6	2.5	1.2	0.45	−1.11	800
2005.01.17	5.1	3.6	1	0.65	−1.21	800
2005.05.15	6.7	4	1.4	0.7	−1.13	875
2005.09.11	10	5.5	1.7	0.93	−1.28	1000
2006.12.14	4.7	1.7	0.7	0.84	−1.4	900

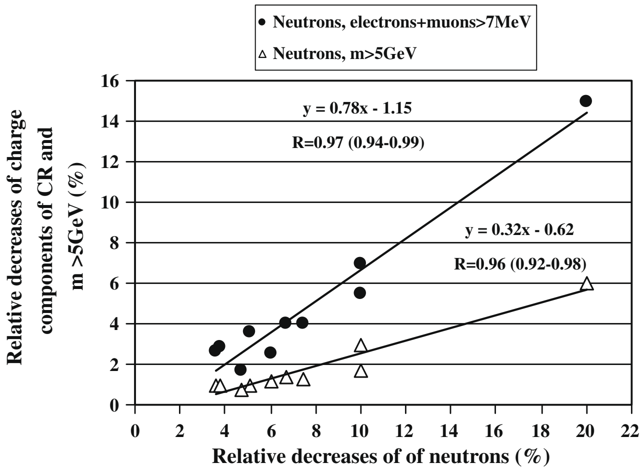

Fig. 2. Relative decreases of the charged CR compared with neutrons.

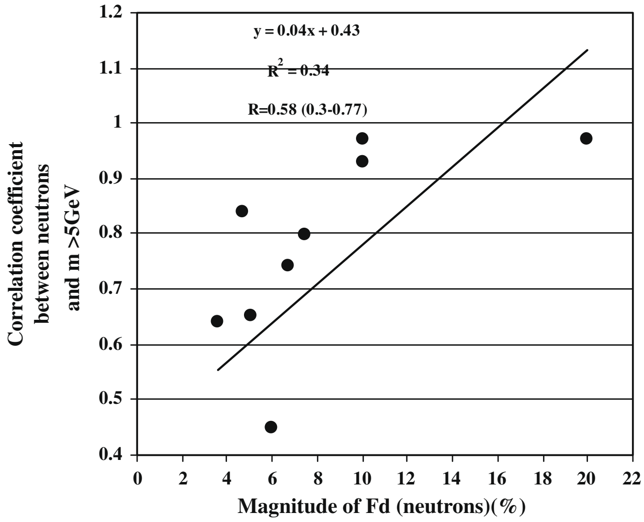

Fig. 3. Dependence of FD magnitude (neutrons) and correlation coefficient between Neutron Monitors and Aragats Multichannel Muon Monitor (>5 GeV muons) time series.

corresponding ICMEs. We select data from three ASEC monitors covering a large range (7–40 GeV, columns 2–4) of the primary proton energies. Correlation coefficients are calculated at FD attenuation phase by 1-min time series for intervals of 5–10 h (by 300–600 points), column 5. In column 6 we post the index of the fitted power function dependence of FD magnitude on the primary energy. The power function fit was done for three points correspondent to FD magnitude in fluxes of neutrons, low energy charge particles and muons with energies above 5 GeV, as it is demonstrated in the Fig. 5. In the last seventh column the maximal solar speed from 1-min data measured by instruments SWEPAM, ACE and SOHO is posted.

In Fig. 2 we can see the relative decreases in different secondary fluxes (neutrons, low energy charged particles, muon with energies greater than 5 GeV) for selected FD events. As it is expected, the relative decrease of definite species of secondary cosmic rays is inversely proportional to the most probable energy of primary generating this species. The most pronounced FD is observed on October 29, 2003 in neutron flux (~20%) and lowest – in >5 GeV muon flux (~6%).

The correlation matrix of the largest detected FD of cycle #23 on October 29, 2003 is posted in Table 2. We can see strong correlations between the neutrons and >5 GeV muon fluxes (most probable energies of primary protons ~7 and ~40 GeV, respectively). ICME having originated the FD on October 29, 2003 was so huge that it equally influenced the GCR flux at least till energies up to 40 GeV. In the scatter plot of the FD magnitude and the correlation coefficient between neutron and >5 GeV muon fluxes (Fig. 3) we can notice a trend, showing growing correlation coefficients for FDs with large magnitudes.

Another possible parameter characterizing the FD strength is the functional dependence of the relative magnitude on the most probable primary energy. In Fig. 4 the dependence of the FD magnitude (for events of 29 October 2003 and 27 July, 2004) of the different secondary cosmic-ray species (neutrons, charged particles and muons with energies greater than >5 GeV) was approximated by the power function. We can see that quality of fit is very high, that allows to use the power index of the dependence as a parameter to characterize the FD strength. In Fig. 5 we post the scatter plot of spectral indices calculated for the FDs from Table 1 vs magnitude of FD in charged component (we use only events in which all the three mentioned fluxes were observed). Although scattering of points is rather large, obviously larger FDs are correspondent to the biggest indices (weaker dependence of FD magnitude on the primary energy).

Table 2
Correlation matrix of time series of different secondary fluxes measured by ASEC on 29 October 2003.

Type of facility	ANM	NANM	SNT Thr0	SNT Thr 1	SNT Thr 2	SNT Thr 3	SNT Thr 4	Muons >5 GeV
ANM	1							
NANM	1.00	1						
SNT Thr 0	0.99	0.99	1					
SNT Thr 1	0.99	0.99	1.00	1				
SNT Thr 2	0.99	0.99	0.99	1.00	1			
SNT Thr 3	0.98	0.98	0.99	0.99	0.99	1		
SNT Thr 4	0.98	0.98	0.99	0.99	0.99	0.99	1	
Munos > 5 GeV	0.97	0.97	0.97	0.97	0.97	0.96	0.95	1

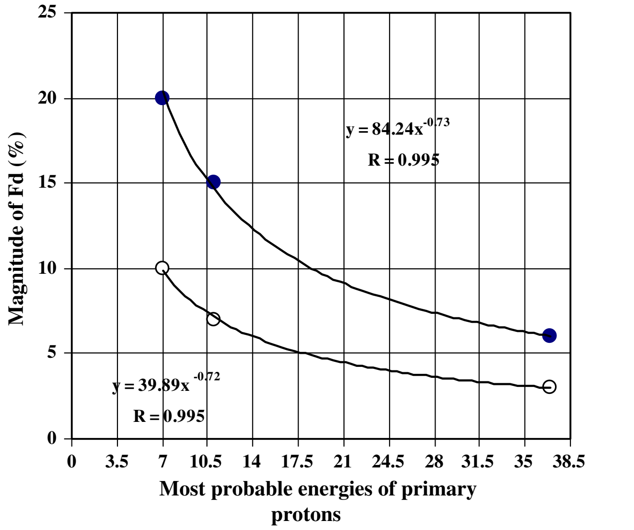

Fig. 4. Dependence of the magnitude of Forbush decrease on the primary energy.

3. Joint analysis of FD with the Moscow Engineering – Physics Institute Muon Detector data

The muon count rate variations during some of the FDs of the 23rd solar cycle were registered by muon detectors DECOR, TEMP and URAGAN operating in the experimental complex NEVOD (MEPhI, Moscow, Barbashina et al., 2007). MEPhI data can path the gap between low energy charged particles and high energy muons (>5 GeV) measured by ASEC. In Table 3 and Fig. 6 we present the data on a FD, which occurred on May 15, 2005. In Fig. 6 we see good agreement for data obtained by detectors located at different latitudes and altitudes. It is evident that FD magnitude in the high energy muon flux measured on the Earth's surface is global characteristic, approximately the same for the different detector locations.

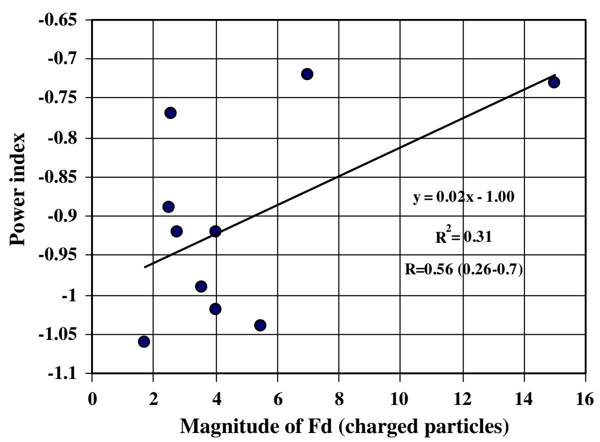

Fig. 5. Dependence of the FD magnitude (in charged secondary flux) and the value of the power index.

Table 3
Magnitudes of FD detected at15 May 2005 by MEPhI and ASEC.

	Median energies of primary (GeV)	Magnitude of FD (%)
Moscow NM	10	7.3
ANM	15	6.7
Charged ANI	24	3.8
URAGAN	23	3.3
TEMP	28	2.8
DÉCOR	50	2.2
AMMM	60	1.34

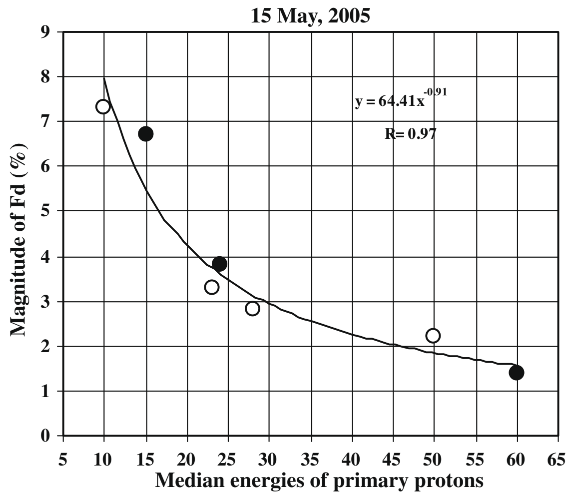

Fig. 6. Observation of the FD from 15 May 2005 by MEPhI. Open symbols – MEPhI data, close symbols – ASEC data.

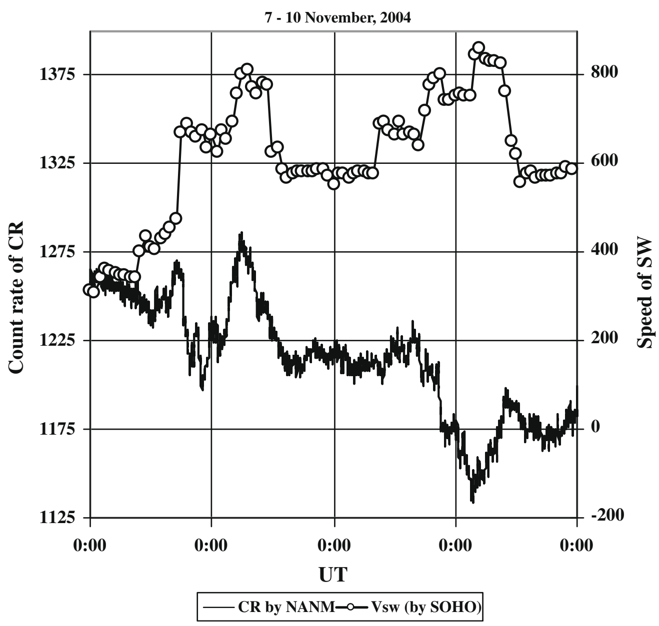

Fig. 7. Several successive ICMEs and geomagnetic storm prevents reliable estimation of the ICME siz.

4. Relation of the FD magnitude to the ICME parameters

The attenuation of the GCR flux due to approaching ICME is dependent on its speed, size, the field strength, and the orientation as well as on the pre-shock conditions of the Interplanetary Magnetic Field (IMF). Most of these parameters are rather difficult to measure and interpret; therefore, the explanation of the FD still lacks many details. For instance, it is rather difficult to estimate the spatial elongation of the ICME. The standard technique of measuring ICME thickness is based on the detection of the region with low proton temperature in solar wind passing ACE and SOHO spacecraft and simultaneously – the mean speed of solar wind (V_{sw}, see Richardson and Cane, 1995; Gopalswamy, 2007). However, this method is not applicable for the multiple colliding ICMEs; cases of the disturbed IMF by previous ICMEs, etc. The method we use is similar to the described one, with the difference that the time of ICME passage is estimated by the duration of FD decreasing phase (from the start of count rate decrease until maximal decrease). Both methods meet difficulties to distinguish successive ICMEs, as an example let's consider the FD occurred at ~18:00 on November 7, 2004, see Fig. 7. At this time the solar wind speed enhanced by ~200 km/s and the neutron count rate started to decrease. However, both count rate and solar wind speed changes are rather complicated, showing several peaks and dips. Therefore, estimation of the size of the ICME is not a simple arithmetic and for reliable estimation we need "clear" events involving a single ICME. The selected standalone ICMEs that generated FDs and allowing estimation of the sizes of ICME are posted in the Table 4. The helio-coordinates of the CME are posted in first column, the date in the second; in the third column we posted the FD magnitude in neutron flux. In columns 3–6 are posted the ICME parameters as measured by ACE spacecraft facilities. Maximal speed of Solar Wind (V_{sw}) and density of solar wind protons are estimated by data from instrument SWEPAM; strength of the magnetic field B_{total} is measured by the MAG facility.

Table 4
"Single" ICMEs generating FD.

The Solar Source of CME	Years, months, days	Relative decrease of neutrons (%)	Maximum speed of SW km/s (by ACE, SOHO)	Jump of density of SW	Jump of B_{total} (nT) by ACE	Durations of decrease phase (h)	L – size of clouds, associated with decrease phase of FD
?	2000.11.26	1.2	435	5	5	–	*
?	2000.11.06	1.3	590	2	7	5	1.1E+07
S15,W15	1998.05.04	1.5	835	13	**36**	–	*
?	2000.08.10	1.6	460	7	5	12	1.9E + 07
N07,W56	2000.02.11	1.7	520	2	6	5	8.4E + 06
N14,W12	2001.03.31	1.9	730	25	**67**	–	*
S07,E89	2003.06.17	1.8	540	2	10	–	*
S17,W40	2000.02.12	2	590	20	18	6	1.2E + 07
N20,E70	1999.09.15	2.4	615	3	11	10	2.1E + 07
N16,W18	2001.10.21	3.1	650	17	12	7	1.4E + 07
N26,W10	2001.08.17	3.8	500	30	28	7	8.8E + 06
N00,E18	2003.11.20	3.8	730	17	**47**	7	1.7E + 07
N10,E08	2004.11.7	3.9	650	40	33	5	1.1E + 07
N17,W31	2001.04.28	4.4	750	9	18	9	2.2E + 07
S21,E31	2001.04.08	4.6	750	13	15	8.5	2.2E + 07
S06,W24	2006.12.14	4.7	900	4	10	4.5	1.4E + 07
N09,W28	2002.09.7	4.8	580	11	20	13	2.4E + 07
S23,E17	2001.10.11	5	550	27	20	8	1.5E + 07
N15,W05	2005.01.17	5.2	800	40	33	8.5	2.2E + 07
N19,W85	2001.04.04	5.4	790	6	15.5	5.5	1.4E + 07
N18,E09	1998.09.24	5.6	810	14	25	6.5	1.40E + 07
N20, E18	2000.06.08	5.5	780	10	19	7	1.9E + 07
N22,W07	2000.07.15	5.9	1000	25	37	7.5	2.7E + 07
N08,W28	2004.11.9	6.4	800	23	29	7	2.0E + 07
N12,E12	2005.05.15	6.7	870	20	42	6	1.8E + 07
S18,E27	2001.04.11	6.7	750	25	29	7.5	1.9E + 07
S16,W12	2001.09.25	6.8	740	22	25	11	2.6E + 07
S23,W09	2004.01.22	7.5	690	15	19	9	2.1E + 07
N06,W18	2001.11.06	9.4	790	30	60	13	3.3E + 07
N04,W30	2004.07.27	10	1035	5	22	5	1.8E + 07
S01,E70	2005.09.11	10	1000	5	20	6	2.2E + 07
S16,E04	2003.10.29	20	1900**	–	52	11.5	5.8E + 07

? – The Solar Source of CME and Solar Wind parameters, impossible to determine.
* Overtake CME.
** Master Data Table of Major Geomagnetic Storms (1996–2005). http://cdaw.gsfc.nasa.gov/geomag_cdaw/Data_master_table.html.

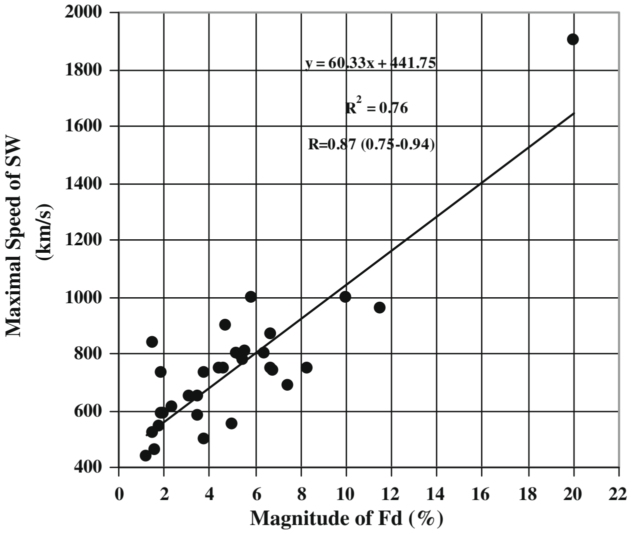

Fig. 8. Dependence of the magnitude of the Forbush decrease on the maximal solar wind speed.

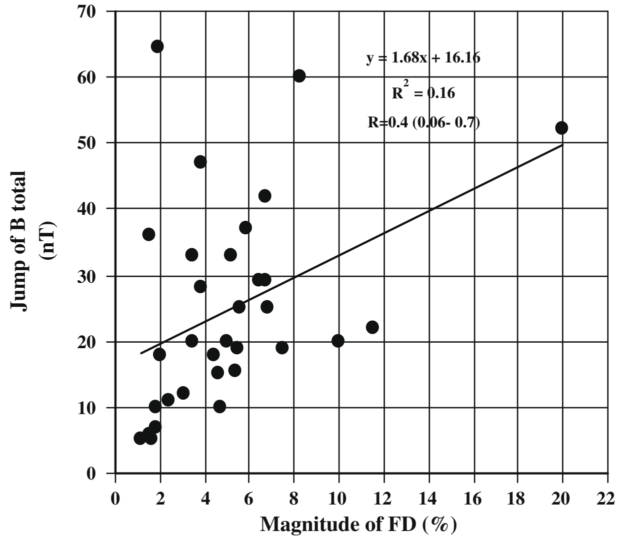

Fig. 10. Dependence of the magnitude of Forbush decrease on the "jump" of the total magnetic field of ICME.

The one and the same procedure was applied to all ICMEs that unleash FD to calculate sizes of ICME; the estimated duration of the FD decreasing phase is posted in the seventh column and corresponding calculated size of IMCE – in the eighth.

Data from Table 4 (total 32 events) was used to investigate correlations between magnitude of FD and ICME parameters. As we can see in Figs. 8 and 9 there is a pronounced dependence between the FD magnitude and ICME speed and size. The dependence of the FD magnitude on the ICME magnetic field (its "jump" at ICME pass) is much weaker (Fig. 10). However, if we exclude the FDs accompanied by strong geomagnetic storms (the depression of CR intensity is someway masked by the reduced cutoff rigidity leading to CR flux enhancement) the discrepancy of points on scatter plot reduces. In Fig. 11 we post the same events as in Fig. 10, excluding events occurred on May 5, 1998, March 31, 2001, and November 20, 2005. The correlation between FD magnitude and change (jump) of total magnetic field measured by MAG facility of ACE spacecraft are notably enlarged. And we did not observe any correlation between FD magnitude and Solar Wind density (Fig. 12).

5. Conclusion

We perform a statistical study of FD decreases detected by the ASEC particle detectors during 23rd solar activity cycle. We present relations of the measured magnitude of FD in different secondary particle fluxes to the most probable energy of the primary protons of GCR that initiated these fluxes. The FD magnitude measured in ASEC during

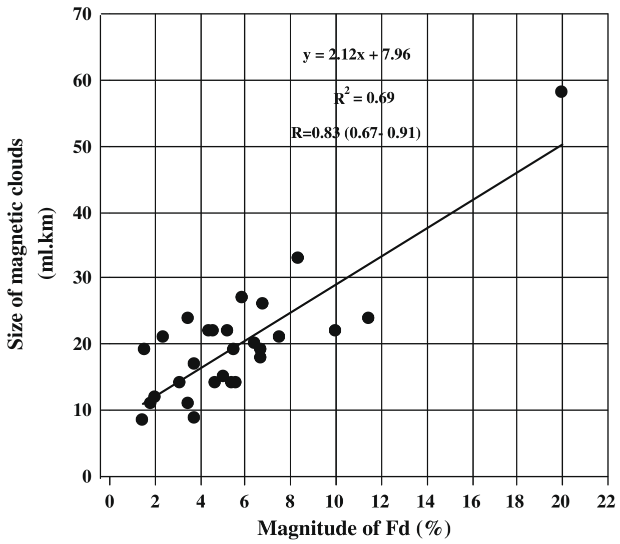

Fig. 9. Dependence of the estimated ICME linear size on the FD magnitude for 28 events.

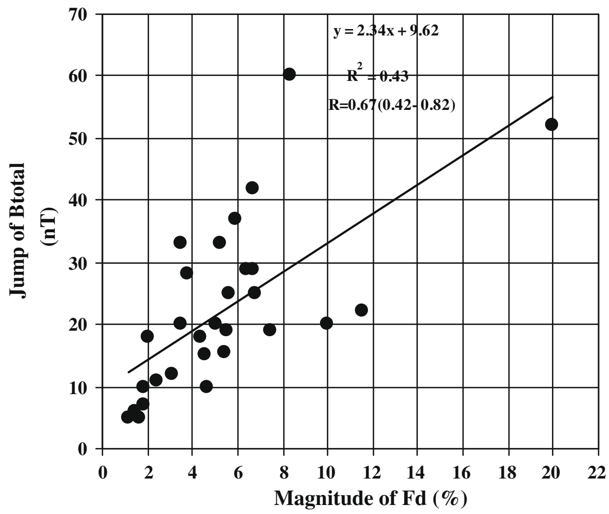

Fig. 11. The same as Fig. 10 without three events excluded (accompanied by severe geomagnetic storms).

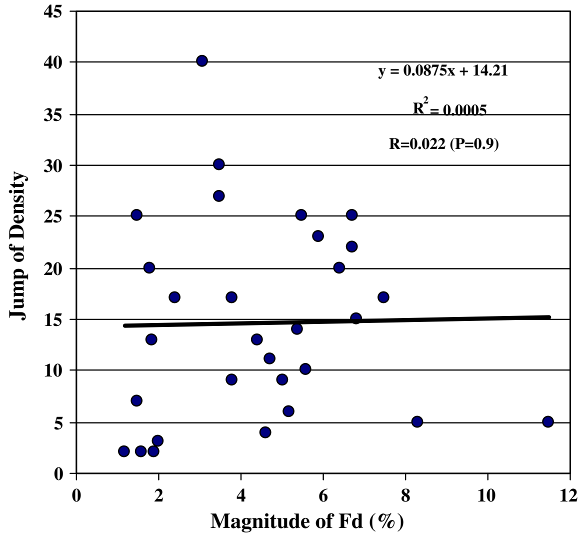

Fig. 12. Dependence of the magnitude of Forbush decrease on the density of solar wind (SW density corresponds to the ICME sheath region.

the 23rd solar activity cycle ranges from about 1.5% to 20% in the secondary neutron flux, 1–15% in the charged low-energy particle flux and 0.6–6% in the >5 GeV muon flux. We introduce two indices to enumerate the ICME "modulation strength", namely: the correlation coefficient of time series of two secondary CR species (neutrons and muons with energies greater than 5 GeV), corresponding to the highest and lowest primary proton energies;

- The power index of the estimated power dependence of the FD magnitude on the most probable energy of primary protons.

Both indices demonstrate apparent positive trend, proving obvious fact that if FD magnitude is large, both low and high energy primaries will be affected by ICME. However, rather large scattering pointed that proposed indices should be calculated by subsamples of events, after applying more specific selection criteria.

Neutron Monitor data was only used for analysis of characteristics of single ICMEs causing Forbush decreases. The modulation strength of the ICMEs is correlated with the speed and size of ICMEs. The correlation with ICME magnetic field can be significantly enlarged if we exclude events accompanied with strong geomagnetic storms. On the base of detected data we cannot claim of existence of any correlation of FD magnitude with density of solar wind.

Acknowledgement

This work was partly supported by ISTC A1554 grant and INTAS 8777 grant. Authors thank N. Gopalswamy and G. Karapetyan for useful discussions and the ASEC staff for providing continuous operation of the particle detectors during the 23rd solar activity cycle.

References

Barbashina, N.S., Dmitrieva, A.N., Borog, V.V. Investigation of Forbush effects in muon flux measured in integral and hodoscopic modes, in: Proc. 30th Intl. Cosmic Ray Conf., vol. 1, pp. 315–318, 2007.

Burlaga, L.F., Chang, G. J. Gephys. Res. 93, 2511–2518, 1988.

Cane, H.V. Coronal mass ejections and Forbush decreases. Space Sci. Rev. 93, 55–77, 2000.

Chilingarian, A., Avakyan, K., Babayan, V., et al. Aragats Space-Environmental Centre: status and SEP forecasting possibilities. J. Phys. G: Nucl. Part. Phys. 29, 939–951, 2003.

Chilingarian, A., Arakelyan, K., Avakyan, K., et al. Correlated measurements of secondary cosmic ray fluxes by the Aragats Space-Environmental Center monitors. NIM A543, 483–492, 2005.

Chilingarian, A., Hovsepyan G. New type of particle detectors for Space Weather research, in: Intl. Symp. on Forecasting of the Radiation and Geomagnetic Storms, Nor Amberd, Armenia, pp. 92–97, 2008.

Forbush, S.F. On the effects in cosmic-ray intensity observed during the recent magnetic storm. Phys. Rev. 51, 1108–1109, 1937.

Forbush, S.F. World-wide changes in cosmic-ray intensity. Rev. Mod. Phys. 11, 168–172, 1939.

Gopalswamy, N. Properties of interplanetary coronal mass ejections. Space Sci. Rev., 2007.

Haurwitz, M.W., Yoshida, S., Akasofu, S.I. Interplanetary magnetic field asymmetries and their effects on polar cap absorption effects and Forbush decreases. J. Geophys. Res. 70, 2977–2988, 1965.

Richardson, I.G., Cane, H.V. Regions of abnormally low temperature as signatures of ejecta in the solar wind and their solar cycle dependence, in: Proc. of the 24th ICRC, vol. 4, p. 868, 1995.

Simpson, J.A. Cosmic-radiation intensity-time variations and their origin. Phys. Rev. 94, 426–440, 1954.

Usoskin, I.G., Braun, I., Gladisheva, O.G., et al. Forbush decrease of cosmic rays: energy dependence of recovery phase. J. Geophys. Res. 113, A07102, doi:10.1029/2007JA012955, 2008.

Van Allen, J.A. Scott Ellsworth Forbush, biographical memoirs. Available from: <http://books.nap.edu/html/biomems/sforbush.html>, 1985.

Zazyan, M., Chilingarian, A. Calculations of the sensitivity of the particle detectors of ASEC and SEVAN networks to galactic and solar cosmic rays. Astroparticle Phys., doi:10.1016/j.astropartphys.2009.08.001, 2009.